Water Science

ORIGINAL ARTICLE Open Access

Scour reduction downstream of a sluice gate using stepped basins under submerged hydraulic jump condition

Wail A. Fahmy[1], M. M. Ibrahim[1], Salma A. Nofal[2*] and Eslam El Tohamy[3]

Abstract

This study experimentally examined the performance of pooled stilling basins with positive and negative steps, with and without baffle blocks, for mitigating local scour and enhancing energy dissipation downstream of sluice gates. The study combined 1, 2, and 3 negative steps with 1, 2, 3, and 4 positive steps. Additionally, the experimental setup included the investigation of adding 1, 2, or 3 rows of baffle blocks, with each row configuration being tested at three different vertical height specifications. Experiments were conducted in a 15.6 m long, 0.30 m wide, and 0.468 m deep recirculating flume at Froude numbers 1.0 to 2.0 under a fixed submergence ratio (s_r= 3.3). A 2.0 m long and 0.1 m deep mobile sand bed was installed downstream of the basin. A total of 12 models with 81 test runs, were examined in the laboratory under various flow conditions. Results showed that steeped basin, model C_1 (two negative steps followed by four positive steps), reduced scour by up to 48%. Adding baffle blocks; with the tallest blocks (E_2,$\frac{h_b}{K}$ =1.5) and blockage ratio of 5%, further increased the reduction to 54%. Energy dissipation improved by up to 59% for model B_4 (one negative step followed by four positive steps). Adding single row configurations of baffles with blockage area 5% and relative height ($\frac{h_b}{K}$ =1) provided the most efficient balance between scour reduction and energy loss. Finally, experimental data are used to derive empirical formulas through multiple linear regression analysis.

Keywords Local scour, Submerged hydraulic jump, Negative-step stilling basin, Positive-step stilling basin, Baffle block

Introduction

Hydraulic jumps are a key phenomenon in open channel hydraulics, commonly occurring downstream of spillways, sluice gates, and regulators. Their efficiency in dissipating excess energy largely depends on the tailwater conditions. When the flow rate exceeds the design capacity, the tailwater depth increases, and a submerged hydraulic jump is formed [33, 34]. Under such conditions, the jump often becomes unstable, resulting in severe local scour.

To mitigate these challenges, stilling basins typically employ two principal design strategies. The first, geometric control (structural dissipation), modifies the basin geometry through positive or negative steps to influence the macro-structure of the jump. This approach stabilizes the jump and enhances volumetric energy dissipation by generating a large, stable recirculation zone [17, 26]. The second strategy, local resistance (obstructive dissipation), uses baffle blocks to promote energy loss through localized drag and turbulence [37]. Although blocks are

This article was transferred to Springer Nature after it was peer reviewed & accepted by the previous publisher.

*Correspondence:
Salma A. Nofal
salma_aly2011@yahoo.com; salma.nofal@oi.edu.eg
[1] Civil Engineering Department, Shoubra Faculty of Engineering, Benha University, Cairo, Egypt
[2] Civil Engineering, Water, and Water structure Department, The High institute for Engineering and Technology, Al-Obour, Egypt
[3] Water, and Water Structure Engineering, Faculty of Engineering, Zagazig University, Zagazig, Egypt

effective in shortening the jump length, their efficiency is highly sensitive to geometric parameters [2] and, if improperly designed, may destabilize the flow near the bed. Operational observations [10] further revealed that rapid gate openings before sufficient tailwater development can trigger intense scour. However, under extreme flow conditions, conventional protection systems, such as concrete blocks, gabion walls, and riprap aprons, may be overtopped or eroded. Documented failures at Liscione Dam in Italy [27], Taunsa Barrage in Pakistan [38], and Rio Hondo Dam in Argentina [25] illustrate how severe local scour and high-velocity flows can lead to structural failure within the energy dissipation zone.

Numerous experimental studies [4, 29] have shown that submerged jumps strongly affect scour depth, scour evolution, and energy dissipation efficiency. De Padova et al. [9] provided a comprehensive review of hydraulic jump research, emphasizing the persistent challenges in predicting submerged jump behavior and turbulence modeling. Since submerged jumps are commonly encountered under real field conditions, they provide more practical insights into stilling basin performance. Khalili et al. [21], for instance, demonstrated that submergence intensifies scour and alters the energy dissipation mechanism downstream of sluice gates.

A variety of techniques have been explored to reduce local scour downstream of hydraulic structures. Ohtsu et al. [30] examined the flow behavior downstream of sluice gates with different drop heights, while Armenio et al. [6] and A. Negm et al. [28] analyzed the combined effect of bottom rise and end sills, whereas Oliveto et al. [31] focused on local scour downstream of positive-step basins, showing that both step height and location significantly influence scour characteristics. A. M. Negm et al. [29] further reported that placing a negative step near the gate enhances energy dissipation, while shifting it toward the basin end reduces it. Similarly, A. M. Ali et al. [3] confirmed that multiple positive steps improve energy dissipation and minimize scour. More recent studies [13, 20, 26, 32] have reaffirmed the benefits of negative steps in improving stilling basin efficiency, although their design requires careful consideration of step height and sidewall elevation to prevent surface instabilities.

The application of baffle blocks as energy dissipaters has also been widely investigated. El-Masry et al. [11] highlighted that block height has a greater influence on scour reduction than block position. Habibzadeh et al. [16] reported that energy dissipation in submerged jumps with blocks may exceed that of free jumps, depending on the degree of submergence. Ghaderi et al. [15] analyzed the hydraulic behavior of sills and macro-roughness elements under both submerged and unsubmerged conditions, providing insights into turbulence and drag characteristics. Ghaderi et al. [14] investigated the flow field of submerged hydraulic jumps over triangular macroroughnesses, showing their influence on turbulence and energy dissipation. S. Y. Kumcu et al. [23] compared various dissipater designs in chute channels, while El-Saie et al. [12] demonstrated that scattered square blocks offer a more economical and efficient configuration than circular ones.

Despite these advancements, limited attention has been given to the combined influence of step configuration and baffle blocks in pooled stilling basins under submerged conditions. The present experimental study addresses this gap by investigating how step arrangement and block configuration jointly influence energy dissipation and local scour characteristics. The findings aim to develop analytical expressions incorporating step geometry, block height, and arrangement pattern to support the design of more efficient stilling basins.

Material and methods

The main objective of this study is to experimentally evaluate the hydraulic performance of advanced stilling basins equipped with various step configurations, positive, negative, and combined, on the scour hole geometry downstream of a sluice gate under varying flow conditions. The effectiveness of adding baffle blocks with different shapes (square, cylindrical, and rectangular) to stepped basin is also studied.

Dimensional analysis

Based on the selection of all variables controlling the scour phenomenon downstream of the pooled basin, the dimensionless variables were defined using Buckingham's theory. Figure 1 presents a sectional elevation of the studied problem, with and without baffle blocks**.** The maximum scour depth can be expressed as a function of the governing parameters as follows:

$$D_s = f(B, l_p, X, G, K, h_b, w_b, l_b, , S_b, Y_1, Y_{up}, Y_3, Y_4, V_G, V_1, V_4, D_{50}, \rho, \mu, \rho_s, g) \quad (1)$$

where: B is channel width; L_p is the pooled basin length; X: is the net length of the pooled basin between negative and positive steps; G is the gate opening; K is the pooled basin height; W_b is the block width; L_b is the block length; h_b is the block height;S_b is the spacing between block; D_s is the scour hole depth; Y_{up} is the upstream water level; Y_1

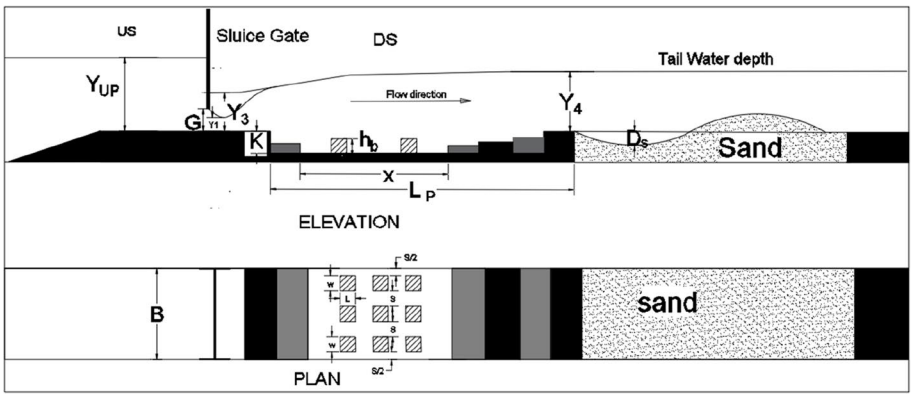

Fig. 1 Definition sketches for the experimental model

is the initial water depth; Y_3 is the back water depth; Y_4 is the depth of water at the end of the submerged jump; D_{50} is the median grain size; g is the gravitational acceleration; V_G is the velocity under gate; V_1 is the velocity at vena contraction; V_4 is the velocity at the end of hydraulic jump; ρ is the mass density of water; μ is the dynamic viscosity of water, and ρ_s is the mass density of soil.

By applying Buckingham's π-theorem and selecting ρ, G, and V_G as repeating variables, Eq. (1) can be expressed in dimensionless form as follows:

$$\frac{Ds}{y_1} = f\left(F_G, R_N, W_e, N_p, N_n, s_r, \varnothing_{area}, \frac{B}{Y_1}, \frac{G}{Y_1}, \frac{K}{Y_1}, \frac{L_p}{Y_1}, \frac{X}{Y_1}, \frac{h_b}{Y_1}, \frac{S_b}{Y_1}, \frac{l_b}{Y_1}, \frac{w_b}{Y_1}, \frac{Y_4}{Y_1}, \frac{Y_{up}}{Y_1}, \frac{\rho_s}{\rho}, \frac{D_{50}}{Y_1}\right) \quad (2)$$

The effects of,$\frac{\rho_s}{\rho}$, and $\frac{D_{50}}{y_1}$ were excluded because only one fluid and one soil. The channel (B), gate opening (G), pooled basin length (L_p), pooled basin height (k), and block dimensions ($L_B = w_b$) were kept constant. The spacing between blocks (s_b) was equal to the block width. The submergence ratio (s_r) was also kept constant. The effect of the Reynolds, $R_N = \frac{V_G X G X \rho}{\mu}$, was neglected, as viscosity has a negligible influence on the characteristics of hydraulic jumps. $w_e = \frac{\rho * {V_G}^2 * G}{\sigma}$, using a surface tension, standard value for clean water at room temperature, coefficient of σ = 0.072 N/m. Weber number is large (We ≫ 1), making viscous and surface tension effects negligible. Therefore, similar to other experimental studies, Reynolds and Weber numbers were omitted in this work as their influence was considered insignificant under the present flow conditions [18].

Hence, Eq. 2 can be reduced to Eq. 3

$$\frac{Ds}{y_1} = f\left(F_G, F_d, N_p, N_n, N_b, \varnothing_{area}, \frac{h_b}{Y_1}, \frac{Y_4}{Y_1}, \frac{Y_{up}}{Y_1}\right) \quad (3)$$

The relative energy dissipated by the jump can also formulated by functional relationship as in Eq. (4):

$$\frac{E_4 - E_3}{E_3} = f\left(F_G, N_p, N_n, N_b, \varnothing_{area}, \frac{h_b}{Y_1}, \frac{Y_4}{Y_1}, \frac{Y_{up}}{Y_1}\right) \quad (4)$$

$$E_3 = Y_3 + \frac{{V_1}^2}{2g} \quad (5)$$

$$E_4 = Y_4 + \frac{{V_4}^2}{2g} \quad (6)$$

where: $\frac{Ds}{y_1}$ is the maximum relative scour depth, $F_d = \frac{V}{(g' x d_{50})}$ is the densimetric particle Froude number with V cross-sectional flow velocity, g' is the modified gravitational acceleration, $g' = \frac{\rho_s - \rho}{\rho_s}$, $F_G = \frac{V_G}{(gxG)^{0.5}}$ is the Froude number under the gate, $V_G = \frac{Q}{BXG^2}$ is the velocity just downstream the gate, N_n is the number of negative steps, N_P is the number of positive steps, N_b is the number of baffle blocks, $\frac{h_b}{Y_1}$ is the relative block height,$\frac{Y_{up}}{Y_1}$: is the relative upstream water level, $\frac{Y_4}{Y_1}$ is the relative sequent water depth, $S_r = \frac{Y_3}{Y_1}$ is the relative submerged water depth, and $\varnothing_{area} (\varnothing_{area} = \frac{N_b * L_b * W_b}{B * X})$ is the area blockage ratio.

Experimental flume setup

The experiments were conducted in the Hydraulic and Water Engineering Laboratory at the Faculty of Engineering, Zagazig University, Egypt. A recirculating laboratory flume of 15.6 m length, 0.30 m width, and 0.468 m depth was used for the trials as shown in Fig. 2. The discharges were measured using a pre-calibrated orifice meter installed in the feeding pipeline. The stilling basin model was made of marble, the steps and blocks were

Fig. 2 A general view of the flume

constructed from wood, as shown in Fig. 3. Pooled basin dimensions: length (L_p), width (B), and depth (K) are 100, 30, and 5 cm, respectively. The dimensions of the pooled basin were adopted from the experimental work of A. M. Negm et al. [29]. The step height (K) should be less than critical height to avoid surface jump in the basin [20]. The tailgate at the end of the flume was used to control the tail water depth. During the experiments, the tailgate was controlled such that the submergence ratio ($S_r = \frac{Y_3}{Y_1}$) was set to 3.3. The submerged hydraulic jump was selected because it frequently occurs downstream of sluice gates under increased tailwater conditions [4, 29].The applied discharges corresponded to Froude numbers ranging from 1.0 to 2.0.

Soil properties of bed material

The removable bed is composed of uniform natural sand, 0.1 m deep and 2.0 m long, formed downstream of the pooled basin. The total length of the movable bed channel used in the present study (2m) is consistent with the channel length employed in the study of Daneshfaraz et al. [8]. The soil has a median diameter d_{50} of 0.66 mm (Fig. 4); the geometrical deviation, $(\sigma g = (\frac{d_{84}}{d_{16}})^{0.5})$ was 2.33, where $d_{50\%}$, $d_{84\%}$, and $d_{16\%}$ represent the sieve openings that allow 50%, 84%, and 16% of the sediment particles to pass, respectively. The sediment used in the downstream erodible bed was uniform sand, characterized by a median grain size of d_{50} of 0.66 mm. The selection criterion was based on previous experimental studies [5]. Using d_{50} ensures reproducibility, simplifies comparison with other research, and reflects the dominant particle size controlling the initiation and development of local scour.

Fig. 3 Plan of the experimental models

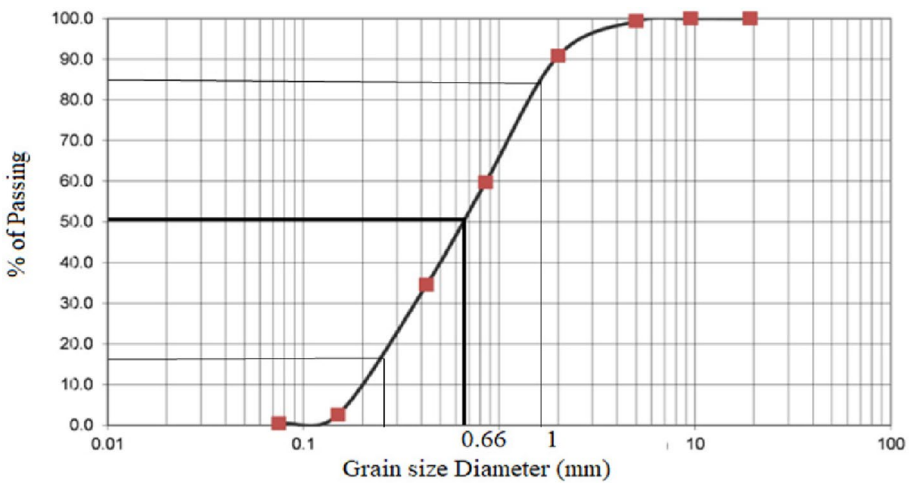

Fig. 4 Particle size distribution for particle bed

Experimental procedure

The experimental procedure was as follows: (1) the sand bed surface was leveled by a plate attached to the carriage; (2) the tested model was fixed in the flume; (3) the gate opening was set at 4.5 cm; (4) the pump was switched on and the required discharge was gradually achieved using the control valve; (5) the tailgate was adjusted to ensure the desired submergence condition was attained; (6) the run time was initiated, and the scour process was observed until complete stability was reached after 120 min which is required to reach 85% of the maximum scour depth, Fig. 5; and (7) the main pump was switched off, and then the tailgate was fully opened to drain the water. After the water was completely drained, the scour hole profile was measured using a point gauge with an accuracy of ± 0.1 mm. The movable bed topography was measured at 5 cm intervals in both the longitudinal (x) and transverse (y) directions to characterize the scour pattern.

The experimental work in this study was carried out over 12 models (Tables 1 and 2), with each set constrained to the same submergence ratio (s_r=3.3), and a range of Froude numbers from 1.0 to 2.0 as detailed below:

(1) Model A (reference case): A flat floor without any steps or baffles was adopted as the baseline for comparison.
(2) Model B (positive and negative step arrangements): Four scenarios were considered, consisting of a single negative step followed by a varying number of positive steps:

- B1: one negative step followed by one positive step.
- B2: one negative step followed by two positive steps.
- B3: one negative step followed by three positive steps.
- B4: one negative step followed by four positive steps.

(3) Model C (multiple negative step arrangements): Two scenarios were examined, including:

- C1: two consecutive negative steps followed by four positive steps.
- C2: three consecutive negative steps followed by four positive steps.

(4) Model D (baffle blocks): Three experimental configurations were carried out using square baffle blocks with a constant relative height ($\frac{h_b}{k} = 1$), while varying the blockage area, one row, two rows, and three rows (D1, D2, and D3).
(5) Model E (block height variation): Another set of experiments was performed with a constant blockage area (∅area = 5%), while varying the relative block height ($\frac{h_b}{K}$=0.5, 1, and 1.5) denoted as models E1, D1, and E2, respectively. Tables 1 and 2 show all the models tested in this study, along with their corresponding shapes

The scale effect

In the present study, some parameters with minor influence were not considered due to the experimental scale. For example, the channel sidewalls were made of Perspex with a smooth surface, so wall friction was negligible compared with the bed resistance. The flume width was selected to be sufficiently larger than the flow depth and the baffle block dimensions, which helped minimize sidewall interference. The use of a submerged hydraulic

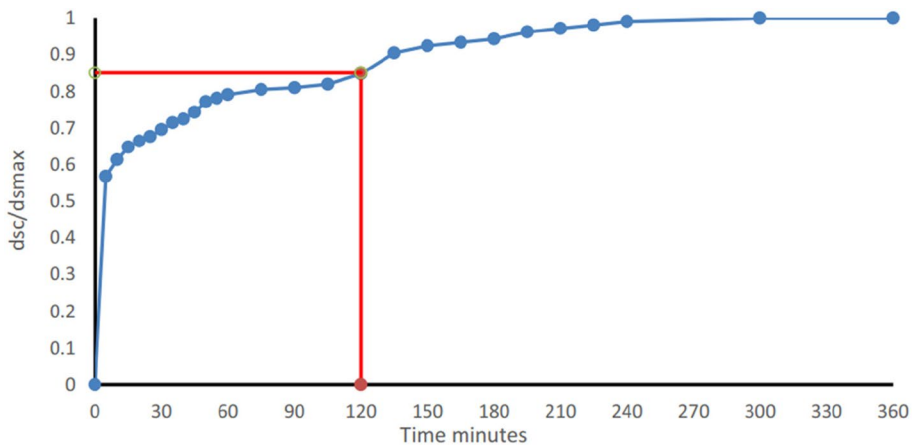

Fig. 5 The time curve of the runs

Table 1 Experimental data

Test No	Model Description	No of negative step	No of positive step	Y_3(m)	F_G	F_d	D_s(m)	$\frac{D_s}{Y_1}$	Y_4(m)	E_3(m)	$E_4(m)$	$\frac{\Delta E}{E_3}\%$
1	*A*: Flat basin	0	0	0.1	1.31	12.1	0.023	0.76	1.39	0.18	0.14	20.84
2				0.1	1.43	13.3	0.030	1.00	1.40	0.20	0.14	26.30
3				0.1	1.56	14.5	0.038	1.26	1.59	0.21	0.16	23.74
4				0.1	1.67	15.5	0.042	1.39	1.60	0.23	0.16	28.63
5				0.1	1.79	16.6	0.053	1.76	1.75	0.25	0.18	28.22
6				0.1	2.01	18.6	0.065	2.16	1.85	0.29	0.19	34.26
7				0.1	2.12	19.7	0.075	2.49	1.89	0.31	0.19	37.46
8	B_1: One positive step	1	1	0.1	1.19	11.0	0.031	1.03	1.34	0.17	0.14	17.39
9				0.1	1.28	11.9	0.033	1.09	1.39	0.18	0.14	19.38
10				0.1	1.31	12.2	0.034	1.13	1.40	0.18	0.14	20.44
11				0.1	1.55	14.4	0.037	1.23	1.50	0.21	0.15	27.33
12				0.1	1.81	16.8	0.042	1.39	1.59	0.25	0.16	34.99
13				0.1	2.02	18.7	0.052	1.72	1.64	0.29	0.17	41.40
14	B_2: Two positive steps	1	2	0.1	1.18	10.9	0.028	0.93	1.26	0.16	0.13	21.28
15				0.1	1.19	11.1	0.029	0.96	1.28	0.17	0.13	20.98
16				0.1	1.31	12.2	0.030	1.00	1.30	0.18	0.13	25.64
17				0.1	1.55	14.4	0.033	1.09	1.40	0.21	0.15	31.71
18				0.1	1.82	16.9	0.038	1.26	1.54	0.25	0.16	37.24
19				0.1	1.98	18.4	0.041	1.36	1.64	0.28	0.17	40.01
20	B_3: Three positive steps	1	3	0.1	1.17	10.8	0.028	0.93	1.30	0.16	0.13	18.65
21				0.1	1.31	12.1	0.030	1.00	1.32	0.18	0.14	24.50
22				0.1	1.34	12.4	0.030	1.00	1.40	0.18	0.14	21.71
23				0.1	1.58	14.6	0.033	1.09	1.55	0.22	0.16	26.26
24				0.1	1.84	17.1	0.037	1.23	1.65	0.26	0.17	34.13
25				0.1	1.94	17.9	0.045	1.49	1.72	0.27	0.18	35.49
26	*B4*: Four positive steps	1	4	0.1	1.16	10.8	0.025	0.83	1.30	0.16	0.13	18.16
27				0.1	1.22	11.3	0.026	0.86	1.35	0.17	0.13	21.44
28				0.1	1.27	11.8	0.026	0.86	1.37	0.18	0.14	20.86
29				0.1	1.43	13.3	0.030	1.00	1.44	0.20	0.14	28.01
30				0.1	1.62	15.0	0.035	1.16	1.50	0.22	0.15	33.13
31				0.1	1.69	15.7	0.036	1.19	1.56	0.23	0.15	33.62
32				0.1	1.95	18.1	0.038	1.26	1.63	0.28	0.16	41.74
33				0.1	2.02	18.7	0.039	1.29	1.74	0.29	0.18	38.21

Table 1 (continued)

Test No	Model Description	No of negative step	No of positive step	Y_3(m)	F_G	F_d	D_s(m)	$\frac{D_s}{Y_1}$	Y_4(m)	E_3(m)	E_4(m)	$\frac{\Delta E}{E_3}$%
34	C_1: two negative step	2	4	0.1	1.15	10.6	0.023	0.76	1.18	0.16	0.12	24.42
35				0.1	1.24	11.5	0.024	0.80	1.20	0.17	0.12	27.47
36				0.1	1.55	14.4	0.030	1.00	1.42	0.21	0.15	30.84
37				0.1	1.67	15.5	0.035	1.16	1.50	0.23	0.16	32.68
38				0.1	1.79	16.6	0.036	1.19	1.58	0.25	0.16	34.47
39				0.1	1.91	17.7	0.037	1.23	1.60	0.27	0.17	38.65
40	C_2: Three negative step	3	4	0.1	1.19	11.0	0.028	0.93	1.30	0.17	0.13	19.73
41				0.1	1.30	12.0	0.028	0.93	1.32	0.18	0.14	23.81
42				0.1	1.50	13.9	0.035	1.16	1.40	0.21	0.14	29.33
43				0.1	1.60	14.8	0.036	1.19	1.52	0.22	0.16	28.51
44				0.1	1.82	16.9	0.038	1.26	1.60	0.25	0.17	35.06
45				0.1	1.91	17.7	0.038	1.26	1.61	0.27	0.17	38.31

Test No	Model Description	No of negative step	No of positive step	No of rows	Relative block height (h/k)	Y_3 (m)	F_G	F_d	D_s (m)	$\frac{D_s}{Y_1}$	Y_4 (m)	E_3 (m)	E_4 (m)	$\frac{\Delta E}{E_3}$
46	D_1: one row block (h/k = 1)	2	4	1	1	0.1	1.14	10.6	0.020	0.66	0.124	0.16	0.13	20.83
47						0.1	1.27	11.8	0.025	0.83	0.13	0.18	0.13	23.66
48						0.1	1.31	12.2	0.025	0.83	0.14	0.18	0.14	20.44
49						0.1	1.47	13.7	0.026	0.86	0.144	0.20	0.15	26.34
50						0.1	1.66	15.3	0.030	1.00	0.156	0.23	0.16	29.50
51						0.1	1.89	17.5	0.033	1.09	0.163	0.27	0.17	36.92
52						0.1	1.91	17.7	0.033	1.09	0.17	0.27	0.18	35.21
53	D_2: Two row blocks	2	4	2	1	0.1	1.15	10.6	0.020	0.66	0.1156	0.16	0.12	25.81
54						0.1	1.22	11.3	0.023	0.76	0.12	0.17	0.12	26.78
55						0.1	1.37	12.7	0.028	0.93	0.13	0.19	0.13	28.12
56						0.1	1.60	14.8	0.032	1.06	0.14	0.22	0.15	33.60
57						0.1	1.77	16.4	0.035	1.16	0.1433	0.25	0.15	39.08
58						0.1	1.82	16.8	0.038	1.26	0.15	0.25	0.16	38.50
59						0.1	1.91	17.7	0.038	1.26	0.16	0.27	0.17	38.65
60	D_3:Three row blocks	2	4	3	1	0.1	1.16	10.8	0.022	0.73	0.118	0.16	0.12	25.08
61						0.1	1.19	11.1	0.025	0.83	0.12	0.17	0.12	25.48
62						0.1	1.38	12.8	0.030	1.00	0.13	0.19	0.13	28.72
63						0.1	1.47	13.7	0.030	1.00	0.14	0.20	0.14	28.19
64						0.1	1.59	14.7	0.035	1.16	0.143	0.22	0.15	31.82
65						0.1	1.67	15.5	0.037	1.23	0.1433	0.23	0.15	35.37
66						0.1	1.83	17.0	0.040	1.33	0.1533	0.26	0.16	37.91
67						0.1	1.94	17.9	0.040	1.33	0.16	0.27	0.17	39.55

Table 1 (continued)

Test No	Model Description	No of negative step	No of positive step	Y_3(m)	F_G	F_d	D_s(m)		$\frac{D_s}{Y_1}$	Y_4(m)	E_3(m)	E_4(m)		$\frac{\Delta E}{E_3}$%	
68	E_1: Block height (h/k = 0.5)	2	4	1	0.5	0.1	1.16	10.7		0.020	0.66	0.12	0.16	0.12	23.82
69						0.1	1.27	11.8		0.020	0.66	0.124	0.18	0.13	26.68
70						0.1	1.47	13.7		0.025	0.83	0.135	0.20	0.14	30.50
71						0.1	1.59	14.7		0.033	1.09	0.15	0.22	0.15	28.82
72						0.1	1.69	15.6		0.036	1.19	0.156	0.23	0.16	31.00
73						0.1	1.79	16.6		0.036	1.19	0.16	0.25	0.17	33.87
74						0.1	1.92	17.8		0.037	1.23	0.163	0.27	0.17	38.09
75	E_2: Block height (h/k = 1.5)	2	4	1	1.5	0.1	1.11	10.3		0.015	0.50	0.13	0.16	0.13	15.70
76						0.1	1.24	11.5		0.020	0.66	0.135	0.17	0.14	19.29
77						0.1	1.37	12.7		0.022	0.73	0.139	0.19	0.14	23.64
78						0.1	1.55	14.4		0.025	0.83	0.139	0.21	0.14	32.15
79						0.1	1.71	15.9		0.030	1.00	0.156	0.24	0.16	31.99
80						0.1	1.87	17.3		0.032	1.06	0.17	0.26	0.18	33.63
81						0.1	1.96	18.2		0.035	1.16	0.177	0.28	0.18	34.91

Table 2 Sketches for the experimental cases

Models	Description	Models	Description
A	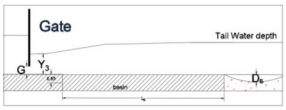	C_2	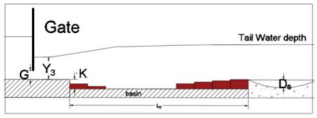
B_1	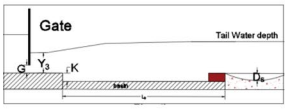	D_1	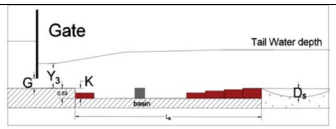
B_2	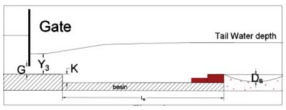	D_2	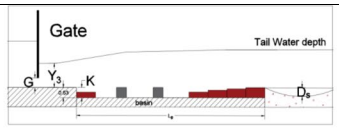
B_3	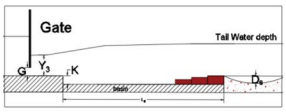	D_3	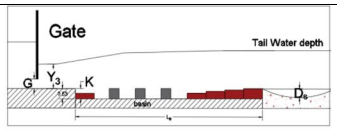
B_4	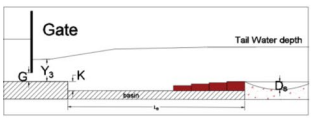	E_1	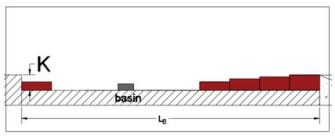
C_1	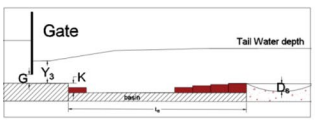	E_2	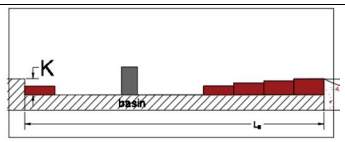

jump also contributed to reducing the sidewall influence by confining a greater portion of the flow vertically.

Analysis and discussion

A total of 81 runs were conducted. The experiments were carried out in four phases: flatbed model and pooled model with positive steps, negative steps, and baffle blocks. The results are analyzed using the gate Froude number (F_G) to achieve the optimal design of the stilling basin depending on the relative energy dissipation ($\frac{\Delta E}{E_3}$) and relative scour depth ($\frac{D_s}{Y_1}$).

Effect of positive steps

The relationship between the relative maximum scour depth ($\frac{D_s}{Y_1}$) and the gate Froude number (F_G) for positive step models B_1, B_2, B_3, and B_4 at $s_r = 3.3$ is shown in Fig. 6. Model B_1 produced the largest values of $\frac{D_s}{Y_1}$, whereas model B_4 produced the smallest. At $F_G = 1.91$, the relative scour depth decreased by 20%, 37%, 31%, and 40% for models *B1, B2, B3*, and *B4*, respectively, compared with the flat model (*A*). These results are consistent with those reported by A. M. Ali and Mohamed [3].

Energy dissipation was also evaluated for the positive-stepped basin (Fig. 7). The relative improvement increased by 57%, 52%, 35%, and 59% for models B_1, B_2, B_3, *and* B_4, respectively, compared with the flat basin (model *A*). This limited effect is attributed to the occurrence of a submerged hydraulic jump, where reduced turbulence and air entrainment significantly lowered the dissipation efficiency. Similar observations were reported by Kumar Jayant et al. [22], Choi et al. [7], and Jahad et al. [19], who confirmed that the limited improvement in energy dissipation in positive-stepped models is due to the submerged hydraulic jump, which is inherently less efficient than a free jump.

Figure 8 shows the scour hole profiles for different tests at a Froude number of 1.91.

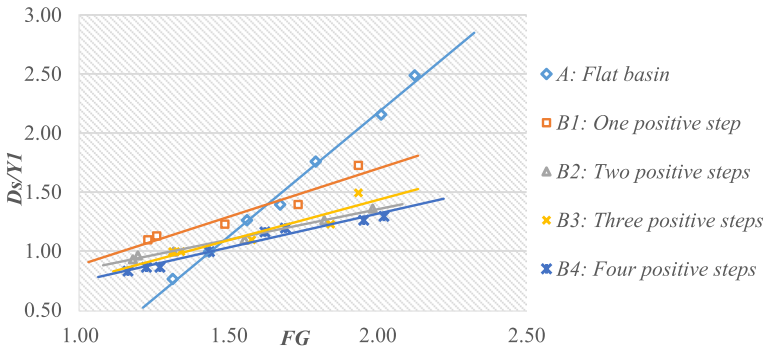

Fig. 6 Relationship between $\frac{D_s}{Y_1}$ and F_G for different models of B1, B2, B3 and B4

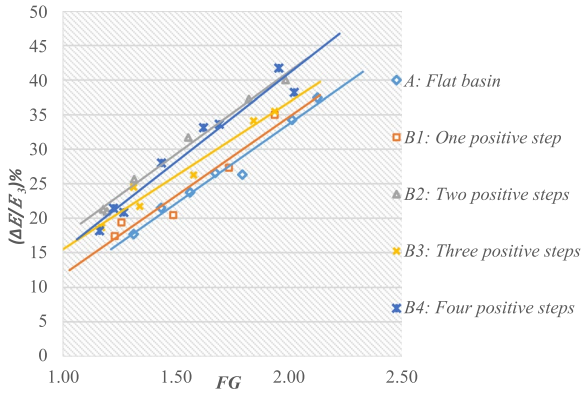

Fig. 7 Relationship between $\frac{\Delta E}{E_3}$ and F_G for different models of B1, B2, B3, and B4

Effect of negative steps

The impact of combining different numbers of negative steps (B_4, C_1, *and* C_2) followed by positive steps on the maximum scour depth was analyzed. Figure 9 shows reductions in maximum scour depth of 40%, 43%, and 48% for models B_4, C_2, *and* C_1, respectively, compared with the flat basin at $F_G = 1.91$. In model B_4, a dead zone formed after the negative step, altering the water flow path and keeping it away from the basin bed. In model C_2, the interaction between the last negative step and the first positive step creates a dead zone in the lower part of the pooled basin, reducing the effectiveness of the negative steps. Model C_1 is proved to be the most effective, as the water flow is directed towards the positive steps, enhancing their impact.

The analysis of energy dissipation indicates that the introduction of steps significantly enhances performance compared to the flat basin, as shown in Fig. 10. Model B_4 achieved the highest improvement, with an increase of 59% in energy dissipation. Models C_1 and C_2 followed, with increases of 47% and 46%, respectively. Although B4 provided the maximum gain, model C_1 can be considered more efficient from a design standpoint, as it combines high energy dissipation with superior scour reduction.

Pazooki et al. [32] showed that the final step height strongly affects the jet trajectory and energy dissipation at the basin entrance. In this study, the same principle was extended by combining negative steps, which create dead zones, with positive steps, which enhance dissipation, resulting in better flow control and reduced scour.

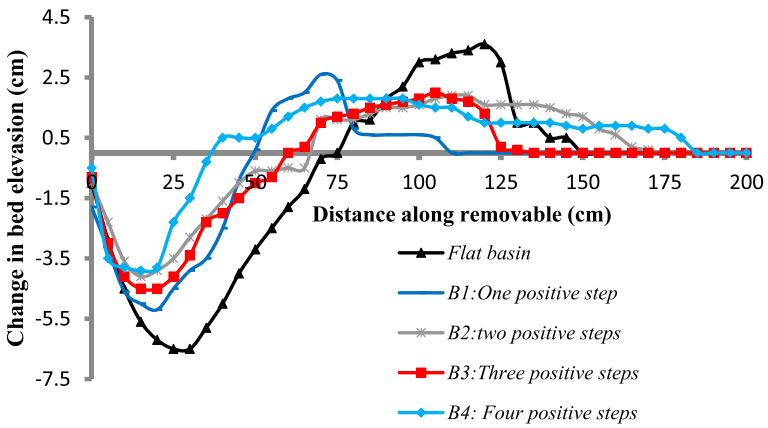

Fig. 8 Effect of step configuration (B_1, B_2, B_3, *and* B_4) on bed elevation change along removable bed and the flat basin model (*A*) at $F_G = 1.91$

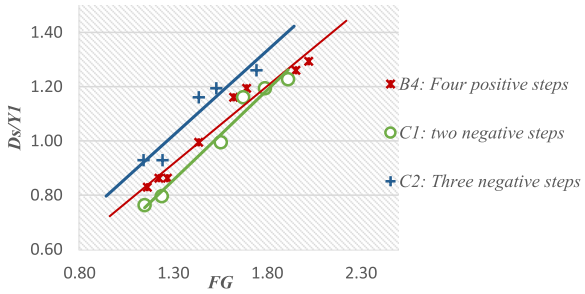

Fig. 9 Relationship between $\frac{D_s}{Y_1}$ and F_G for different models of B_4, C_1, and C_2

Figure 11 presents the scour hole profiles for different tests at Froude number 1.9.

Figure 12 illustrates the flow paths for the different cases involving negative steps.

Effect of baffle blocks

In this case, the experimental data were analyzed based on the relative energy dissipation and relative scour depth to identify the optimal number of baffle block rows (one, two, or three) with different relative heights ($\frac{h_b}{K}$=0.5, 1, and 1.5) installed in a pooled basin with negative and positive steps.

Effect of the block's arrangement

The effect of square blocks in a pooled basin with two negative steps followed by four positive steps was examined under three arrangements (D_1, D_2, and D_3), corresponding to area blockage ratios ($\varnothing_{area} = \frac{N_b * L_b * W_b}{B * X}$) of 5%, 10%, and 15%, respectively, using identical block dimensions (h_b=W_b=L_b=5 cm). The dimensions of blocks were selected in line with recent experimental studies, such as Rasul et al. [36], who used similar block sizes to fit the flume layout and ensure effective energy dissipation.

As shown in Fig. 13, the relative scour depth decreased most significantly with a single row (model D_1), achieving a scour reduction ratio of 49%. This can be attributed to the fact that multiple rows introduce higher turbulence and secondary vortices, which increase sediment mobilization downstream of the basin. These findings are

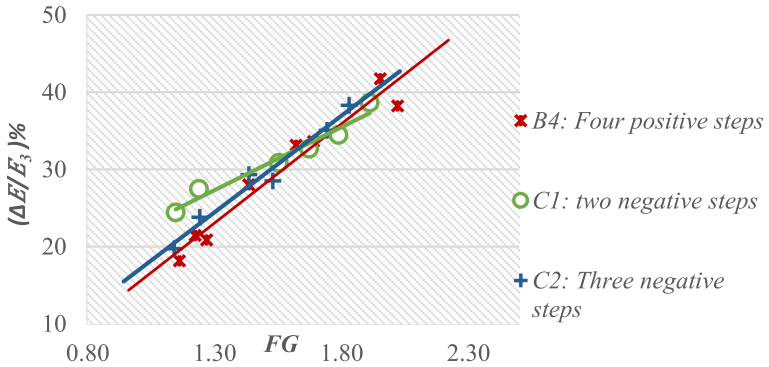

Fig. 10 Relationship between $\frac{\Delta E}{E_3}$ and F_G for different models of B_4, C_1, *and* C_2

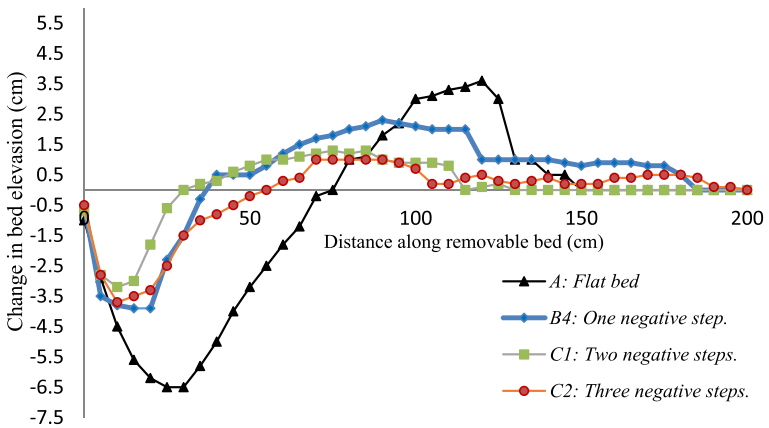

Fig. 11 Relative scour depth versus longitudinal distance beyond stepped basin for shapes B_4, C_1, C_2, and flat basin A at F_G = 1.91

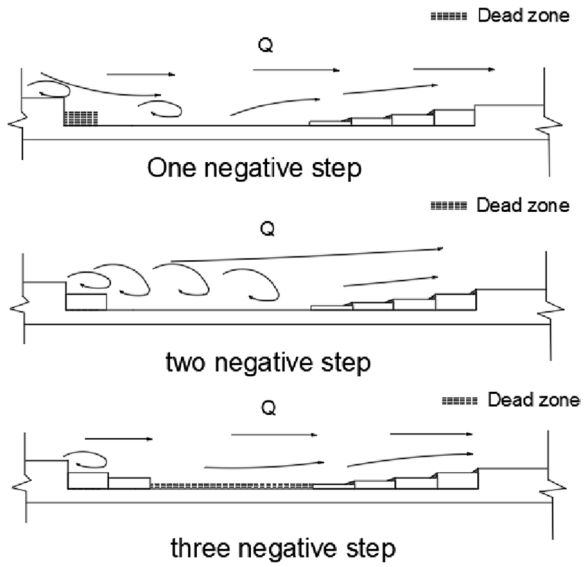

Fig. 12 Flow directions of different negative step models

consistent with earlier studies, which highlighted that the first baffle row has the dominant influence on scour control, while additional rows may not provide further reduction and may even aggravate scour depending on flow and geometry [35, 36].

Figure 14 presents the relative energy dissipation performance of the different layouts. Model D_3 achieved the highest improvement, with an increase of 50%, followed by models D_2 and D_1, which recorded increases of 47% and 34%, respectively. Although D_3 yielded the maximum percentage, model D_1 can be considered more efficient overall, as it combined substantial energy dissipation with the lowest scour depth. According to Ş. Y. Kumcu et al. [24] and Rashed et al. [35], increasing the number of baffle rows enhances turbulence and shear-layer interactions within the basin, thereby improving energy dissipation. However,

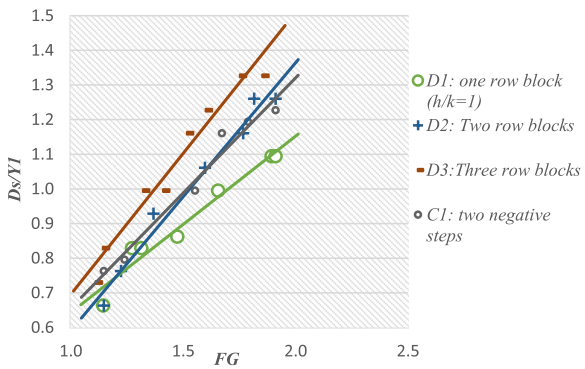

Fig. 13 Relationship between $\frac{D_s}{Y_1}$ and F_G for different models of D_1, D_2, D_3, and C1

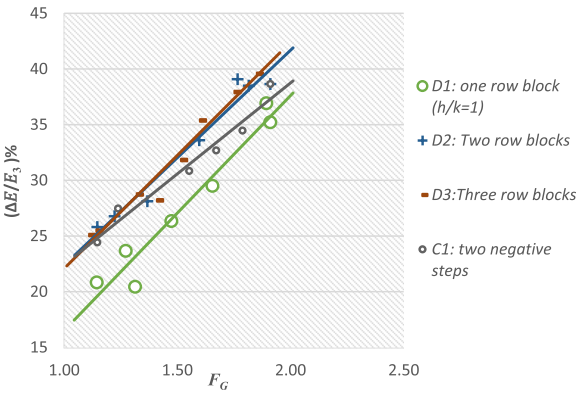

Fig. 14 Relationship between $\frac{\Delta E}{E_3}$ and F_G for different models of D_1, D_1, *and* D_3, *and* C_1

they also emphasized that a single row may in some cases provide superior protection against scour by directly deflecting the jet trajectory and reducing its erosive impact on the bed.

The scour hole geometries under different gate Froude numbers are illustrated in Fig. 15, while Fig. 16 shows the flow patterns generated by the various square block configurations. These visual observations further confirm the dual effect of baffle rows. While additional rows improve dissipation by intensifying turbulence and energy exchange, they also create stronger near-bed recirculation that deepen the scour hole, El-Saie et al. [12]. Consequently, the optimal arrangement depends on achieving a balance between maximizing energy dissipation and minimizing bed erosion.

Effect of block height

In this case, square blocks with one row at different relative heights ($\frac{h_b}{K}$=0.5, 1, and 1.5), models D_1, E_1, and E_2 were used. Figure 17 shows the relationship between relative scour depth and gate Froude number. The results indicate that as the relative block height increased, the relative scour depth decreased, with model E_2 achieving the minimum scour depth, showing a 54% reduction at F_G=1.91. This is because the height of the obstacle directly influences the flow path, slowing the flow velocity and reducing scour.

Figure 18 illustrates the effect on relative energy dissipation. Unlike scour reduction, the highest block (E_2) resulted in lower dissipation efficiency, while the intermediate block height (E_1) achieved the best performance in terms of energy loss. Model E_1 achieved the highest improvement, with an increase of 45%, followed by models D_1 and E_2, which recorded increases of 34% and 33%, respectively. Abdelaal et al. [1] emphasized that the most effective block sill height is close to the critical depth

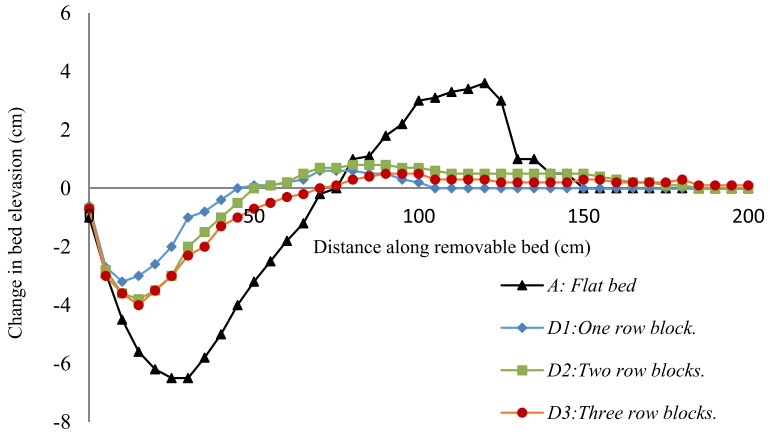

Fig. 15 Relative scour depth versus longitudinal distance beyond stepped basin for shapes D_1, D_2, D_3, and flat basin at $F_G = 1.91$

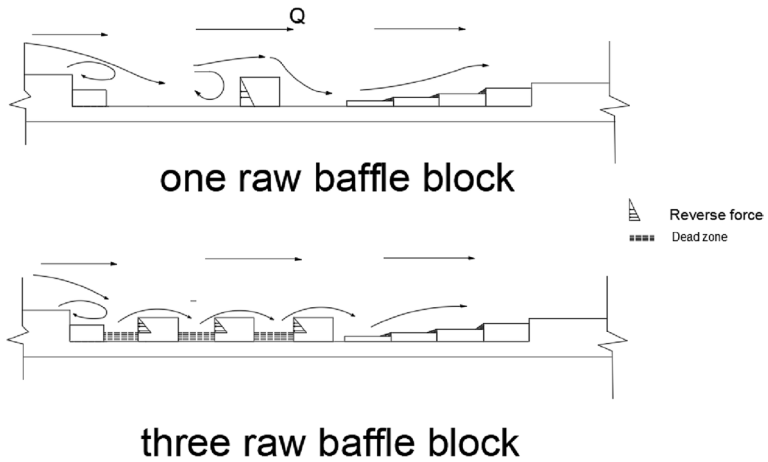

Fig. 16 Flow directions in different configurations of square blocks

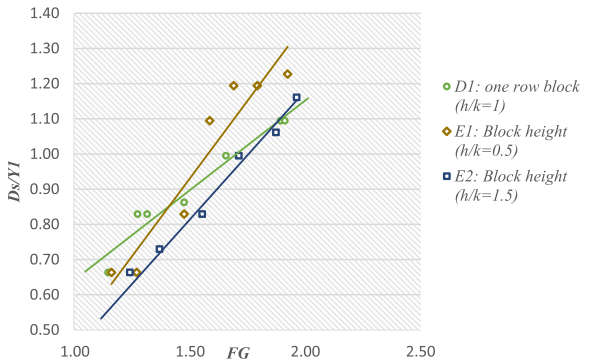

Fig. 17 Relationship between $\frac{D_s}{Y_1}$ and F_G for different models of D_1, E_1, and E_2

($Y_{Critical}$), as excessive heights tend to deflect the jet excessively, reducing turbulence and lowering dissipation efficiency.

Figure 19 presents the scour hole profiles at Froude number 1.91.

Figure 20 illustrates the reduction percentage of relative scour depth for different cases used in this research, compared to the flat bed model at $F_G = 1.91$. The results show that the pooled basin with two negative steps followed by four positive steps (model C_1) reduced the maximum scour depth by 48%. Adding one square row block, corresponding to area blockage ratios ($\varnothing_{area} = \frac{N_b * L_b * W_b}{B * X}$) of 5%, with a relative height ($\frac{h}{K} = 1.5$) to model E_2 increased the scour reduction to 54%.

Prediction of scour hole dimensions

The prediction of the relative scour depth $\frac{Ds}{Y_1}$ downstream of pooled basins with negative steps, positive steps, and baffle blocks was carried out using the current experimental data to develop empirical equations through statistical methods. The scour estimation model was calibrated using 68% of the experimental data and validated

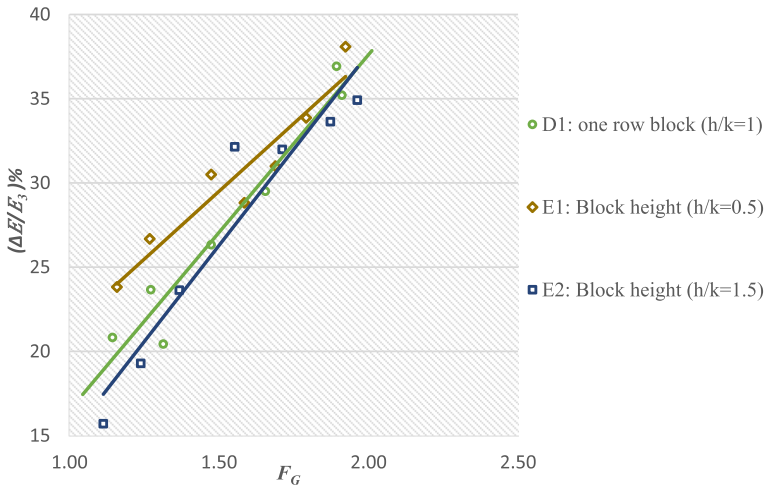

Fig. 18 Relationship between $\frac{\Delta E}{E_3}$ and F_G for different models of D_1, E_1, *and* E2

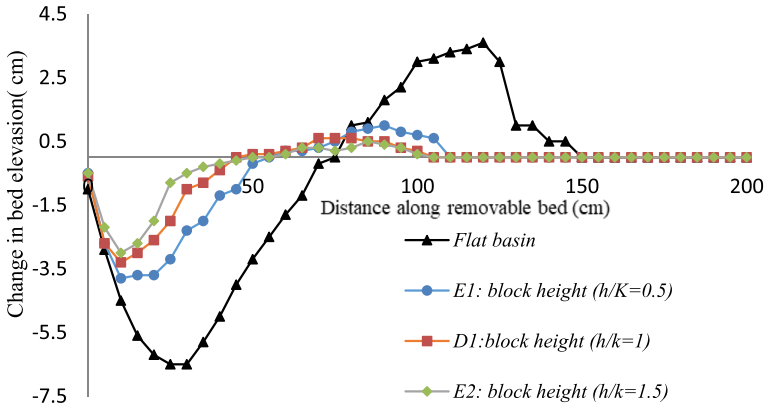

Fig. 19 Relative scour depth versus longitudinal distance beyond stepped basin for shapes E_1, E_2, D_1, and flat basin A at $F_G = 1.91$

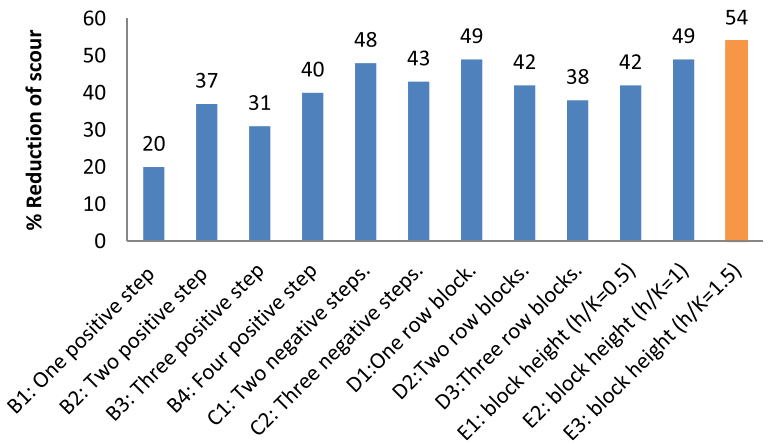

Fig. 20 Reduction percentage of relative scour depths at $F_G = 1.91$

with the remaining 32%. The regression coefficients (C_0, C_1, C_2, C_3, C_4, and C_5) were estimated using the least squares method, based on the datasets of (a) pooled basins with steps and (b) pooled basins with both steps and blocks (Table 3). Substituting the obtained regression coefficients into Eq. (7) yielded Eq. (8) for case (a) and Eq. (9) for case (b). The equations are applicable only within the tested discharge range and structural configurations (positive steps, negative steps, and baffle blocks). Parameters such as Reynolds and Weber numbers were neglected due to their minor influence at the model scale. Therefore, the proposed relations should be applied cautiously and are not directly generalizable to prototype-scale conditions without further verification.

$$\frac{D_s}{Y_1} = C_0 + C_1F_G + C_2N_n + C_3N_p + C_4N_r + C_5(\frac{h_b}{K}) \quad (7)$$

Comparison of Eq. 7 with the measured data is shown in Fig. 21 for both cases (a) and (b). The prediction of Eq. 7 shows fair agreement in both cases, confirming the reliability of the developed empirical equations.

$$\frac{D_s}{Y_1} = 0.2 + 0.436xF_G + 0.035xN_n - 0.057xN_p \quad (8)$$

where: $\frac{Ds}{y_1}$ is the maximum relative scour depth, F_G is the gate Froude number, N_n is the number of negative steps, N_p is the number of positive steps, N_r is the number of rows, and $(\frac{h_b}{K})$ is the relative block height.

Limitations and future works

- Scale effects: Laboratory scale under Froude similarity may not fully capture prototype sediment transport and turbulence.
- Testing conditions: Limited step heights, block configurations, and sediment sizes were examined.
- Sidewall influence: Some lateral effects may still have influenced scour patterns.
- Sediment simplification: Uniform sand was used, unlike natural mixed or cohesive beds.
- Future work: Numerical and field-scale studies under wider hydraulic and sediment conditions are recommended to validate the equations and support practical design guidelines.

Conclusion

This study experimentally investigated the effect of positive steps, negative steps, and baffle block arrangements and heights on local scour and energy dissipation

$$\frac{D_s}{Y_1} = 0.166 + 0.4475xF_G + 0.0363xN_n - 0.0557xN_p + 0.0454xN_r - 0.124x\,(\frac{h_b}{K}) \quad (9)$$

Table 3 Coefficients of Eq. 7

Case	C_0	C_1	C_2	C_3	C_4	C_5	Multiple R	R square	Standard error
(a)	0.2	0.436	0.035	−0.057	-	-	0.957	0.916	0.0469
(b)	0.166	0.4475	0.0363	−0.0557	0.045	−0.124	0.967	0.935	0.0413

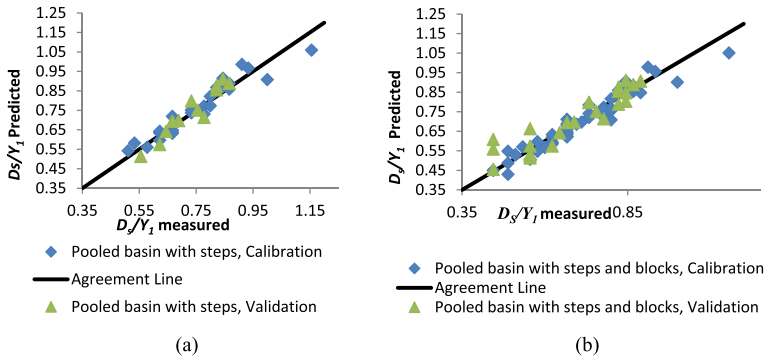

Fig. 21 Comparison between the measured and predicted data for the equation. **a** Pooled basin with steps, and **b** pooled basin with steps and blocks

downstream of pooled basins. The findings can be summarized as follows:

The inclusion of positive steps significantly reduced scour depth compared to the flat basin, with reductions of up to 40%. Among the tested layouts, model B_4 (one negative step followed by four positive steps) proved most effective in mitigating scour.

Combining negative steps with positive ones further enhanced scour reduction. Model C_1 (two negative steps followed by four positive steps) achieved the greatest scour mitigation (48% reduction), as the flow was better directed toward the positive steps. While model *B4* provided the highest dissipation gain (59%), C_1 offered a better balance between scour control and energy loss.

Introducing square blocks into the pooled basin showed that a single row (model D_1) minimized scour depth most effectively (49% reduction), while multiple rows increased turbulence and aggravated scour despite enhancing dissipation. Model D_3, with three rows, achieved the highest energy dissipation (50%), but D_1 provided a more efficient balance between dissipation and scour control.

Increasing block height consistently reduced scour, with the tallest block ($E2$, $\frac{h_b}{k} = 1.5$) yielding the minimum scour depth (54% reduction). However, energy dissipation peaked at the intermediate height ($E1$, $\frac{h_b}{k} = 0.5$), achieving a 45% improvement.

Nomenclature

B Channel bed width (L)
L_p Pooled basin length (L)
XNet basin length between negative and positive steps (L)
Y_{up} Upstream water level (L)
Y_1Initial water level (L)
Y_3 Backwater depth (L)
Y_4 The depth of water at the end of the submerged jump(L)
G Gate opening (L)
K Pooled basin height (L)
w_b Block width (L)
L_b Block length (L)
h_b Block height (L)
S_b Block spacing (L)
$\varnothing_{area}$ The area blockage Ratio (-)
D_{50} Median grain size (L)
D_s Scour hole depth (L)
s_r Submergence ratio (-)
ρ Mass density of water (ML^{-3})
μ Dynamic viscosity of water ($ML^{-1}T^{-1}$)
ρ_s Mass density of water (ML^{-3})
V_G The velocity under gate (LT^{-1})
V_1 The velocity at vena contration (LT^{-1})
V_4 The velocity at end of hydraulic jump (LT^{-1})
F_G Gate Froude's number (-)
F_d the densimetric particle Froude number with V cross-sectional flow velocity (-)
$g^{'}$ modified gravitational acceleration (LT^{-2})
w_e Webber number (-)

Authors' contributions

Salma A. Nofal performed the experimental work, data analysis, and manuscript preparation. All authors; Wail A. Fahmy, M. M. Ibrahim, and Eslam El-Tohamy; reviewed and approved the final manuscript.

Funding

No funding was received for this study.

Declarations

Competing interests

No potential conflict of interest was reported by the author.

Received: 15 June 2025 Accepted: 2 November 2025
Published online: 11 March 2026

References

1. Abdelaal GMM, et al. Effect of perforated inclination and height of sill on maximum scour depth and energy losses downstream a sluice gate. Egypt Int J Eng Sci Technol. 2024;47(1):25–32.
2. Abdelhaleem FSF. Effect of semi-circular baffle blocks on local scour downstream clear-overfall weirs. Ain Shams Eng J. 2013;4(4):675–84.
3. Ali AM, et al. Effect of stilling basin shape on the hydraulic characteristics of the flow downstream radial gates. Alexandria Eng J. 2010;49(4):393–400.
4. Ali HM, et al. Minimizing downstream scour due to submerged hydraulic jump using corrugated aprons. Ain Shams Eng J. 2014;5(4):1059–69.
5. Alwan HH, et al. Evaluation of local scour development downstream an apron of different angles for an ogee spillway. Kufa J Eng. 2016;7(3):1–12.
6. Armenio V, et al. On the effects of a negative step in pressure fluctuations at the bottom of a hydraulic jump. J Hydraul Res. 2000;38(5):359–68.
7. Choi S, et al. Longitudinal change in flow structures and energy loss of free jumps and submerged jumps of flows over an embankment-type weir. KSCE J Civ Eng. 2024;28(3):1084–93.
8. Daneshfaraz R, et al. Experimental investigation of scouring parameters of the downstream bed of simple and gabion rostral drops. AQUA—Water Infrastruct Ecosyst Soc. 2025;74(4):335–48.
9. De Padova D, et al. Hydraulic jump: a brief history and research challenges. Water. 2021;13(13):1733.
10. Edward AE. Hydraulic energy dissipators: New York. Toronto, London: McGraw Hill Book Co., Inc; 1959.
11. El-Masry A, et al. Minimization of scour downstream heading-up structure using a single line of angle baffles. Eng Res J Helwan Univ ã. 2000;69. https://www.researchgate.net/publication/283600649_Minimization_of_scour_downstream_heading-up_structure_using_a_single_line_of_angle_baffles?__cf_chl_rt_tk=L1zmIt2f64FASmddOkUn8.RZhVuitXezhd6lKKp0Y7Y-1768894120-1.0.1.1-rPxFs1WdyJ4wV84g9G7erETTsUFeBid_h9nhwi.0z9A.
12. El-Saie Y, et al. Performance of using advanced stilling basin as an energy dissipation by using three-dimensional numerical model. Egypt Int J Eng Sci Technol (EIJEST). 2024;46(1). https://www.researchgate.net/publication/373149853_Performance_of_Using_a_Special_Stilling_Basin_as_an_Energy_Dissipation_by_Using_Three-Dimensional_Numerical_Model
13. Eroğlu N, et al. Local energy losses for wave-type flows at abrupt bottom changes. J Irrig Drain Eng. 2020;146(9):04020029.

14. Ghaderi A, et al. Numerical simulations of the flow field of a submerged hydraulic jump over triangular macroroughnesses. Water. 2021;13(5):674.
15. Ghaderi A, et al. Characteristics of free and submerged hydraulic jumps over different macroroughnesses. J Hydroinformatics. 2020;22(6):1554–72.
16. Habibzadeh A, et al. Exploratory study of submerged hydraulic jumps with blocks. J Hydraul Eng. 2011;137(6):706–10.
17. Hager WH, et al. Hydraulic jumps at positive and negative steps. J Hydraul Res. 1986;24(4):237–53.
18. Heller V. Scale effects in physical hydraulic engineering models. J Hydraul Res. 2011;49(3):293–306.
19. Jahad UA, et al. Flow characteristics and energy dissipation over stepped spillway with various step geometries: case study (steps with curve end sill). Appl Water Sci. 2024;14(3):60.
20. Jiang L, et al. Investigation of a negative step effect on stilling basin by using CFD. Entropy. 2022;24(11):1523.
21. Khalili AM, et al. Experimental investigation of submerged hydraulic jump downstream of sluice gate in erodible channel. Paper presented at the Proc. of the 13th International Congress on Civil Engineering, Tehran. 2023.
22. Kumar Jayant H, et al. Numerical study of submerged hydraulic jumps over triangular macroroughnesses. J Hydroinformatics. 2024;26(1):51–71.
23. Kumcu SY, et al. Experimental and numerical modeling of various energy dissipater designs in chute channels. Appl Water Sci. 2022;12(12):266.
24. Kumcu ŞY, et al. The effect of various energy dissipator layouts on energy dissipating along the stilling basin. J Int Environ Appl Sci. 2023;18(4):145–53.
25. Lopardo RA, et al. Unconventional interpretation of local scour downstream a large dam stilling basin. Paper presented at the First International Conference on Scour of FoundationsInternational Society of Soil Mech and Foundations. 2002.
26. Macián-Pérez JF, et al. Numerical modeling of hydraulic jumps at negative steps to improve energy dissipation in stilling basins. Appl Water Sci. 2023;13(10):203.
27. Moroni M, et al. Numerical and physical modeling of Ponte Liscione (Guardialfiera, Molise) dam spillways and stilling basin. Hydrology. 2022;9(12):214.
28. Negm A, et al. Theoretical modeling of hydraulic jumps at bottom rises in radial stilling basins with end sills. 2004.
29. Negm AM, et al. Hydraulic characteristics of submerged flow in non-prismatic stilling basins. MEJ-Mansoura Eng J. 2021;28(1):19–31.
30. Ohtsu I, et al. Transition from supercritical to subcritical flow at an abrupt drop. J Hydraul Res. 1991;29(3):309–28.
31. Oliveto G, et al. Local scour downstream of positive-step stilling basins. J Hydraul Eng. 2009;135(10):846–51.
32. Pazooki P, et al. Effect of changing the height of final step of the stepped chute on the flow profile in stilling basin using the VOF method. Appl Water Sci. 2020;10(7):1–9.
33. Peterka AJ. Hydraulic design of stilling basins and energy dissipators: United States Department of the Interior, Bureau of Reclamation. 1964.
34. Rajaratnam N. Hydraulic jumps. Adv Hydrosci. 1967;4:197–280. Elsevier.
35. Rashed RE, et al. Effect of hollow semi-circular baffles arrangement on local scour downstream hydraulic structures. MEJ Mansoura Eng J. 2022;47(3):22–31.
36. Rasul AM, et al. Experimental investigation of baffle configurations, blockage, and flow variability on downstream scour in box culverts. Appl Water Sci. 2025;15(5):109.
37. Wu S, et al. Effect of baffles on submerged flows. J Hydraul Eng. 1995;121(9):644–52.
38. Zaffar MW, et al. Numerical investigation of scour downstream of diversion barrage for different stilling basins at flood discharge. Sustainability. 2023;15(14):11032.

Publisher's Note